

# The Effect of Stator Outer Diameter and Length on the Performance of Three-Phase Induction Motor at Constant Volume

İbrahim Çelik<sup>1</sup> , Yüksel Oğuz<sup>1</sup> , M. Caner Aküner<sup>2</sup> 

<sup>1</sup>Department of Electrical Electronics Engineering, Afyon Kocatepe University, Faculty of Technology, Afyonkarahisar, Türkiye

<sup>2</sup>Department of Mechatronic Engineering, Marmara University, Faculty of Technology, İstanbul, Türkiye

**Cite this article as:** İ. Çelik, Y. Oğuz and M. C. Aküner, "The effect of stator outer diameter and length on the performance of three-phase induction motor at constant volume," *Electrica*, 25, 0124, 2025. doi: 10.5152/electrica.2025.24124.

## WHAT IS ALREADY KNOWN ON THIS TOPIC?

- The volume of induction motor components directly impacts material usage and cost.
- The ratio of motor stack length to stator outer diameter significantly affects motor efficiency and performance.
- Optimization techniques are widely utilized for improving motor designs to balance performance and material usage.

## WHAT THIS STUDY ADDS ON THIS TOPIC?

- This study demonstrates how varying the stator outer diameter and stack length at a constant steel sheet volume influences the efficiency and mechanical power of three-phase induction motors.
- By employing surrogate optimization (SO) and advanced simulation tools,

### Corresponding author:

İbrahim Çelik

### E-mail:

ibrahimcelik@aku.edu.tr

**Received:** September 5, 2024

**Revision Requested:** October 6, 2024

**Last Revision Received:** October 15, 2024

**Accepted:** November 22, 2024

**Publication Date:** January 20, 2025

**DOI:** 10.5152/electrica.2025.24124



Content of this journal is licensed under a Creative Commons Attribution-NonCommercial 4.0 International License.

## ABSTRACT

For induction motors covering the vast majority of the industry, the bulk package volume determines the amount of raw material used, i.e., its cost. In this study, the effect on motor performance is investigated by changing the stator outer diameter and motor length without changing the amount of steel sheet. While designing a low-power induction motor, other motor parameters except the motor stack length and stator outer diameter were calculated analytically, and the stator outer diameter and stack length were obtained using the surrogate optimization (SO) technique. The electric motor modeled with the obtained values was analyzed using Maxwell. In this context, the mechanical power of the designed motor was primarily determined as 1.1 kW. A three-phase induction motor is designed for the considered 1.1 kW of mechanical power. The stack package volume of this motor is calculated as 1340.89 cm<sup>3</sup>. This motor stack package volume also indicates the amount of steel sheet to be used. Therefore, the effect on motor performance is investigated by changing the stator outer diameter and length of the motor without changing the amount of steel sheet. The number of stator and rotor poles of the motor is 36 and 28, respectively. As a result of the analysis, an efficiency value of 80.30% is obtained for the case where the  $K_d$  value, which expresses the ratio of the motor stack length to the stator outer diameter, is 0.113.

**Index Terms**—Analysis, design of an electric machine, induction motor, surrogate optimization.

## I. INTRODUCTION

Induction motors (IM), particularly squirrel cage induction motors, are widely used in various sectors, including domestic, commercial, and industrial applications, due to their versatility and reliability. The squirrel cage rotor construction is favored for its simplicity, robustness, and low cost, which contribute to its widespread adoption across industries. The design's durability ensures minimal maintenance, while its cost-effectiveness makes it accessible for various applications, from household appliances to heavy-duty industrial machinery. Moreover, high-efficiency motors have become increasingly important in modern applications, as they reduce energy consumption and minimize environmental impact by requiring fewer raw materials during manufacturing. This focus on energy efficiency aligns with global sustainability goals, driving industries to adopt more eco-friendly solutions. To ensure these motors meet the required standards for industrial use, performance tests, and efficiency classifications are regulated by established standards [1]. These standards provide guidelines for evaluating critical performance parameters, including load capacity, starting torque, temperature rise, and voltage range, ensuring that motors operate reliably and efficiently under varying conditions [2-5].

The design of electrical machines is a complex process that draws upon knowledge from various scientific fields. These include fundamental principles of physics, in-depth studies of electromagnetism, and an understanding of thermal dynamics, mechanical engineering, and even acoustics. Each of these fields plays a crucial role in the overall design process, influencing the machine's performance, efficiency, and reliability [6-8]. For instance, physics provides the foundation for understanding energy conversion processes, while electromagnetism governs the operation of

a comprehensive analysis of motor performance is provided for a 1.1 kW motor design.

- The findings highlight the critical role of the  $K_d$  ratio in optimizing motor performance, offering a new perspective for efficient motor design in low-power applications.

the motor's magnetic fields and interactions [9]. Thermal studies are essential for managing heat dissipation, ensuring that the machine operates within safe temperature ranges, and preventing damage due to overheating [10]. Mechanical aspects are critical for the structural integrity and durability of the motor, particularly in high-stress industrial environments [11]. Acoustics, although sometimes overlooked, is important for minimizing noise levels, which is a key consideration in environments where noise pollution is a concern.

Designing an induction machine, in particular, is a highly intricate and multivariate problem because it requires the integration of these diverse fields. Engineers must account for numerous factors, balancing competing priorities and adhering to strict physical constraints [12, 13]. This involves performing complex statistical calculations to optimize the machine's performance while meeting requirements such as efficiency, durability, and cost-effectiveness. Moreover, the design process is iterative, often requiring multiple rounds of simulation, testing, and refinement to achieve the desired outcome [14]. The result is a carefully engineered product that meets the specific demands of its intended application while adhering to industry standards and regulations.

Developments and demands in automotive technology have created the need for producing more efficient electric or hybrid vehicles. Induction or permanent magnet motors are largely used in commercially produced electric vehicles [15, 16]. While an electric vehicle must operate with constant torque to climb and take off on a slope, constant power must be produced at different speeds while the vehicle is in motion. A study is carried out to increase the constant power region over a wider range [17]. The effects of leakage and magnetization inductance in the constant power region are investigated [18].

The dimensions of the stator slot, rotor slot, and core parts have a great influence on the performance of the IM [19-21]. It is observed that the efficiency and power factor of the IM increased with the increasing the core axial length [22-24]. The stator slot is effective in increasing motor efficiency and reducing the harmonic losses in the stator [25]. It is seen that the torque value of the motor increased by optimizing the physical parameters of the rotor housing [26, 27]. It has been suggested that the rod winding heats less and achieves higher efficiency than the knitted winding [28].

In this study, the ratio between the stator outer diameter and the motor length is changed by keeping the volume of the motor stack package constant, and the effect of this ratio on the motor performance is investigated. The stator outer diameter value was calculated using the Surrogate optimization algorithm to maximize the efficiency value of the motor. While the stator outer diameter value has been increased, the motor length has been reduced in a quadratic ratio. On the other hand, other physical parameters of the motor are kept constant. The effect of this change on motor performance is investigated.

## II. DESIGN OF THREE-PHASE INDUCTION MOTOR

This title explains the calculation of the physical parameters of a 1.1 kW induction motor and its analysis. The power value of the motor to be designed is determined as 1.1 kW, and the physical parameters of the motor are calculated analytically. The frequency of the stator and the number of dipoles, which are other important parameters for the motor, are determined as 4 and 50 Hz, respectively.

### A. The Calculation of Induction Motor Physical Parameters

#### 1) The Stator Parameters

While calculating the basic stator parameters, the  $S_{gap}$  value is calculated first. A few parameters must be determined beforehand to calculate other physical parameters for the induction motor. Efficiency ( $\eta$ ) and power factor ( $\cos\phi$ ) are required to be 80% and 0.83, respectively. Considering these values, when the air gap power ( $S_{gap}$ ) is calculated as in (1), the  $S_{gap}$  value is obtained as 1656.6 VA.

$$S_{gap} = \frac{P}{\eta \cdot \cos\phi} \quad (1)$$

Where  $P$  expresses the mechanical power of the motor. The ratio of the stator length to the stator spring of each pole is called the stack aspect ratio ( $\lambda$ ). It is seen that the stack aspect ratio is in the range of 0.5–2.5 [29-31]. Therefore, it is selected that  $\lambda$  is 1.2. Fig. 1 shows Esson's constant versus air gap power. Esson's constant, the volume utilization factor, is obtained as 135  $\text{j}/\text{dm}^3$  from the graph in Fig. 1.

All necessary parameters are obtained to calculate the stator bore diameter ( $D_{is}$ ) with the equivalence in (2). So,  $D_{is}$  is 80.5 mm.

$$D_{is} = \sqrt{\frac{2p}{\pi \cdot \lambda} \cdot \frac{p}{f} \cdot \frac{S_{gap}}{C_0}} \quad (2)$$

The  $D_{is}$  and lambda, the ratio of the rotor stack length to the arc length of each pole, are known. So, the stator stack length is 75.8 mm. The pole arc length ( $\tau$ ) is obtained by dividing the stator bore circle length by the number of poles. Thus,  $\tau$  is calculated as 63.2 mm.

The number of stator slots ( $m \cdot q$ ) for each pole can be 6 or 9, where  $m$  expresses the number of phases. In this study,  $q$  is 3. A larger  $q$  value generally affects motor performance positively and causes a decrease in harmonics and losses [32]. The stator slot's arc length ( $\tau_s$ ) is obtained by dividing each phase's stator pole arc length by the number of stator slots. Thus, the arc length for the stator slot is obtained as 7 mm. For motors below 100 kW, it is seen that the ratio of the stator's inner diameter ( $D_{is}$ ) to the outer diameter ( $D_{os}$ ) is approximately 0.6 [33-35]. Considering the literature, this ratio is 0.53. Note that  $D_{os}$  is obtained by dividing the  $D_{is}$  value by the said ratio, so  $D_{os}$  is 150.05 mm. Another important parameter in motor performance is the air gap ( $g$ ) value between the stator and rotor. The second equivalence in (3) is used for the calculation of  $g$  as  $2p = 4$ . Note that  $g$  is calculated at approximately 0.3 mm. If this value is too large, it negatively affects motor efficiency and power factor, while it positively affects air gap field harmonics and additional losses.

$$g = \begin{cases} 0.1 + 0.02\sqrt[3]{P_n} & 2p = 2 \\ 0.1 + 0.012\sqrt[3]{P_n} & 2p \geq 2 \end{cases} \quad (3)$$

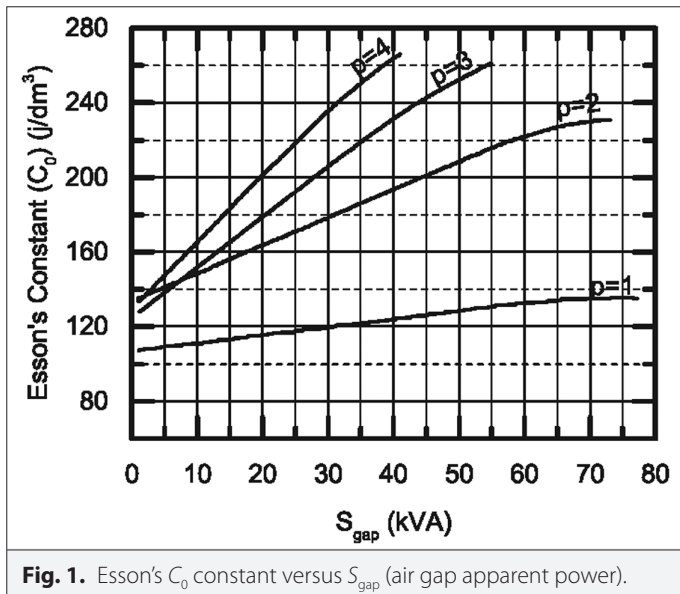


Fig. 1. Esson's  $C_0$  constant versus  $S_{gap}$  (air gap apparent power).

## 2) The Calculation of Stator Winding and Stator/Rotor Slot

In induction motors, stator winding design is made to distribute to the slots the coils of the phases and to determine the current directions of the coils in the slots. For this reason, parameters such as the number of turns and slots must be calculated. The stator slots represent the parts where the coils will be wound. Therefore, the total number of stator slots is obtained by multiplying the number of stator slots ( $m \cdot q$ ) for each pole and the total number of poles. The total number of stator slots is 36. Regarding the winding of the coils in these slots, the stator winding coefficient ( $k_w$ ) is 0.90.

Flux density in the air ( $B_g$ ) is one of the important parameters for electrical machines. For this value, 0.7 T is considered the initial value. However, in the following sections,  $B_g$  is calculated according to the number of turns. Fig. 2 shows form factor  $k_f$  and flux density shape factor  $\alpha_i$  versus teeth saturation.

The tooth saturation coefficient ( $K_{sd}$ ) is selected as 0.4, and the polar spread coefficient ( $\alpha_i$ ) and form factor ( $k_f$ ) corresponding to the  $K_{sd}$  value from Fig. 2 are obtained at 0.729 and 1.085, respectively. The polar flux ( $\phi$ ) is calculated by (4) and is 2.4 mWb.

$$\phi = \alpha_i \cdot \tau \cdot L \cdot B_g \quad (4)$$

The number of turns ( $W$ ) for each phase is calculated by (5) and is 556.14 turns/phase. The number of conductors per slot,  $ns$ , is calculated by dividing  $W$  by the product of the number of pole pairs and  $q$ .  $ns$  is 92.69 turns/slot. That value must be an even number as there are two different coils per slot in a couple of layer winding;  $ns$  is taken 92. When  $W$  and  $B_g$  are calculated according to the new  $ns$  value, they are obtained as 552 and 0.705 T, respectively.

$$W = \frac{V_{ph}}{\frac{2\pi}{\sqrt{2}} \cdot k_f \cdot k_w \cdot f \cdot \phi} \quad (5)$$

Note that the stator nominal current ( $I_n$ ) is calculated by dividing the mechanical power value by the nominal voltage value, efficiency, and power factor values. It is obtained that  $I_n$  is 3.60 A. If high efficiency is desired at the power mentioned above and speed level,

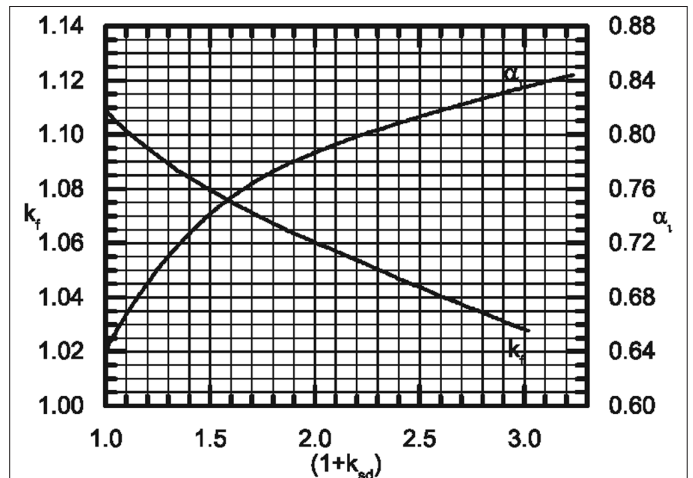


Fig. 2. Form factor  $k_f$  and flux density shape factor  $\alpha_i$  versus teeth saturation [11].

the winding losses dominate the wire's current density ( $J$ ). Therefore, the  $J$  value is 4 A/mm<sup>2</sup>. The magnetic wire cross-section ( $A_{wire}$ ) is calculated as 0.900 mm<sup>2</sup> by dividing the nominal current value by the current density. Since the cross-sectional area of the wire is known, the wire diameter ( $D_{wire}$ ) is easily calculated. Thus, the wire diameter is found to be 1.02 mm.

There are two separate windings in the slot. The occupancy coefficient ( $k_{fill}$ ) is 0.35–0.4 for motors below 10 kW for each phase, while it is taken between 0.4–0.44 for motors above 10 kW. It is chosen to be 0.4. The area of each stator slot ( $A_{slot}$ ) is calculated in (6) and found to be 199.38 mm<sup>2</sup>.

$$A_{slot} = \frac{\pi \cdot d_{wire}^2 \cdot a \cdot n_s}{4 \cdot k_{fill}} \quad (6)$$

The number of parallel branches ( $a$ ) is 1, and some stator slot parameters  $B_{s0}$  and  $H_{s0}$  are chosen as 1 and 1 mm, respectively.

The constant, which is the expression of the influence of lamination insulation thickness for 0.5 mm thick lamination ( $k_{fe}$ ), is 0.96, and rotor tooth flux density ( $B_r$ ) is 1.55 T. The stator slot's tooth width ( $b_s$ ) is calculated as 3.22 mm (7). Note that the sum of  $B_{s1}$  and  $b_s$  of the stator equals one thirty-sixth of the arc of the circle passing through  $B_{s1}$  in Fig. 3.  $B_{s1}$  is calculated as 4.39 mm considering that.

$$b_x = \frac{B_g \cdot \tau_x}{k_{fe} \cdot B_x} \quad (7)$$

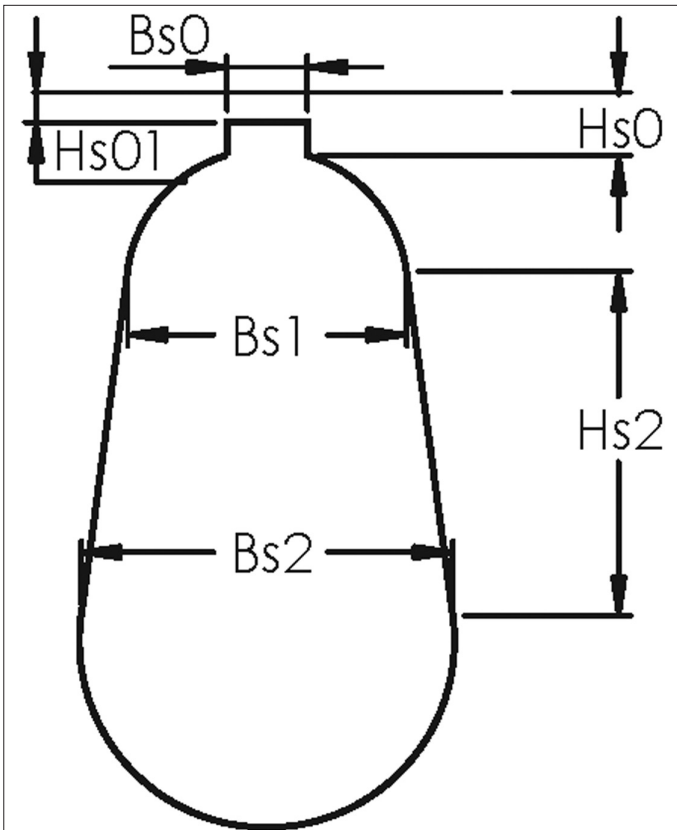


Fig. 3. Physical parameters of the stator/rotor slot.

Two separate equations containing  $H_{s2}$  and  $B_{s2}$  can be written. These are equations of the stator slot area and the arc length of the circle passing through  $B_{s2}$ . These two equations are solved, and  $B_{s2}$  and  $H_{s2}$  are obtained as 8.88 mm and 24.24 mm, respectively. The current ( $I_{bar}$ ) passing through the short-circuit bars of the rotor is calculated as 337.45 A using (8).

$$I_{bar} = \frac{k_r \cdot 2 \cdot m \cdot k_r \cdot W \cdot I_n}{N_r} \quad (8)$$

The ratio of stator mmf to rotor mmf ( $k_r$ ) and the occupancy coefficient of the rotor ( $k_r$ ) are 0.864 and 0.901, respectively.  $N_r$  expresses the number of rotor slots. Since the rotor short-circuit bar is made of aluminum, its current density ( $J_r$ ) is less than that of copper wire.  $J_r$  is 3.42 A/mm<sup>2</sup>. The rotor slot area is 96.67 mm<sup>2</sup> by dividing  $I_{bar}$  by  $J_r$ . By proportioning the rotor outer arc length to the number of poles, the pole arc length ( $\tau_p$ ) for each phase is obtained as 9 mm. The rotor pole flux density coefficient ( $B_r$ ) is 1.60 T. The rotor slot's tooth width ( $b_r$ ) value is 4.11 mm in (7). Some rotor slot parameters  $B_{s0}$ ,  $H_{s0}$ , and  $H_{s01}$  are chosen as 1, 1, and 0.1 mm considering the parameters in Fig. 3, respectively. Note that the sum of  $B_{s1}$  and  $b_r$  of the rotor equals one twenty-eighth of the arc of the circle passing through  $B_{s1}$  of the rotor.  $B_{s1}$  is calculated as 4.16 mm. Considering the rotor slot area equations and the arc length of the circle passing through  $B_{s2}$  on the rotor,  $B_{s2}$  and  $H_{s2}$  are obtained as 0.1 and 18.52 mm, respectively.

### 3) Optimisation of Stator Out Diameter

Optimization is a series of statistical mathematical calculations that allow finding the best input parameter to maximize or minimize the output of a system. In the study, the surrogate optimization technique is used to find the best stator outer diameter parameter that will maximize motor efficiency [36-37]. The mentioned technique tries to minimize the system output. Therefore, motor losses are determined as the output of the system. The method is terminated after 200 iterations. Table I gives the  $D_{os}$ ,  $L$ , and  $K_d$  values obtained by the optimization technique.

where  $K_d$  represents the ratio of the stator's inner diameter to its outer diameter. While increasing  $D_{os}$ , the  $L$  decreases in a quadratic ratio. As a result, the volume of the motor stack package is not changed.

## III. RESULTS AND DISCUSSION

The analyses are made by keeping the volume of the motor stack constant. Table 1 presents the operation conditions of IM for each  $D_{os}$  obtained by SO. This algorithm tries to minimize the output of the plant. Therefore, as shown in Fig. 4, SO converges its output to the minimum by making multiple attempts for the system input. Fig. 4 gives the convergence curve of the Surrogate optimization algorithm for total loss minimization. All parameters in the analysis are constant except those corresponding to  $D_{os}$ . It is seen that decreased  $L$  and  $K_d$  values occur due to increased  $D_{os}$ .

With the increase of  $D_{os}$  value, the  $L$  is shortened. Thus, the stator's inner surface area is reduced. Fig. 5 shows the stator phase current versus speed and  $D_{os}$  value. This event means that the flux path decreases. Therefore, it is observed in Fig. 5 that as the stator's inner surface area decreases, the motor's starting current increases. When the  $D_{os}$  value increases by 100% from 150 to 300 mm, the motor's starting current increases by 140% from 1.457 to 3.503 A.

**TABLE I.** STATOR OUTER DIAMETER, LENGTH, AND  $K_d$

State	$D_{os}$ (mm)	L (mm)	$K_d$
1	152.343	73.563	0.483
2	153.515	72.444	0.472
3	154.687	71.350	0.461
—	—	—	—
99	247.207	27.938	0.113
—	—	—	—
198	297.656	19.270	0.065
199	298.828	19.120	0.064
200	300.000	18.970	0.063

In electric motors, current and loss values are directly proportional. Fig. 6 shows the total loss versus motor speed and  $D_{os}$  value. For this reason, it is seen in Fig. 6 that the increase in the starting current causes an increase in the stator copper losses, and the decrease in the flux path causes an increase in iron losses. When the  $D_{os}$  value increases by 100% from 150 to 300 mm, the motor's total loss increases by 212% from 278.80 to 870.43 W.

As  $L$  decreases, the wire path gets shorter, and the stator stack surface area increases. As the wire path is shortened, stator copper losses are reduced. When the  $L$  value decreases by 74% from 73.563 to 18.97 mm, the motor's efficiency increases by 5.39% from 76.2 to 80.3%. Afterward, as the  $D_{os}$  increases, the motor efficiency decreases. Fig. 7 shows each operating condition's motor efficiency value versus speed. Considering that the motor stack package is of constant weight for all operating conditions, it can be said that the cases are approximately the same in terms of motor cost. Therefore, the state with the highest efficiency can be selected.

Fig. 8 shows the highest efficiency value of the motor at each operating condition corresponding to  $D_{os}$  obtained by SO. The most

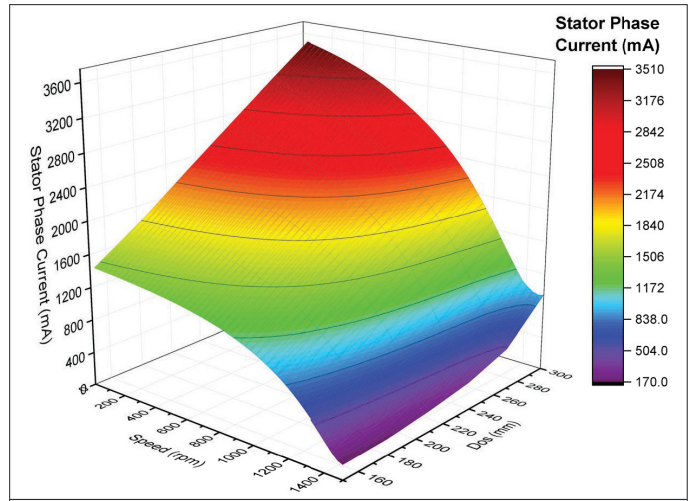


**Fig. 5.** Stator phase current versus speed and  $D_{os}$  value.

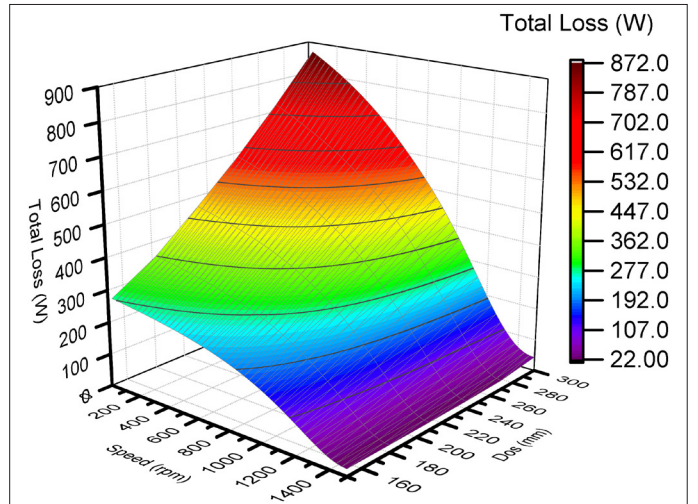


**Fig. 6.** Total loss versus speed and  $D_{os}$  value.

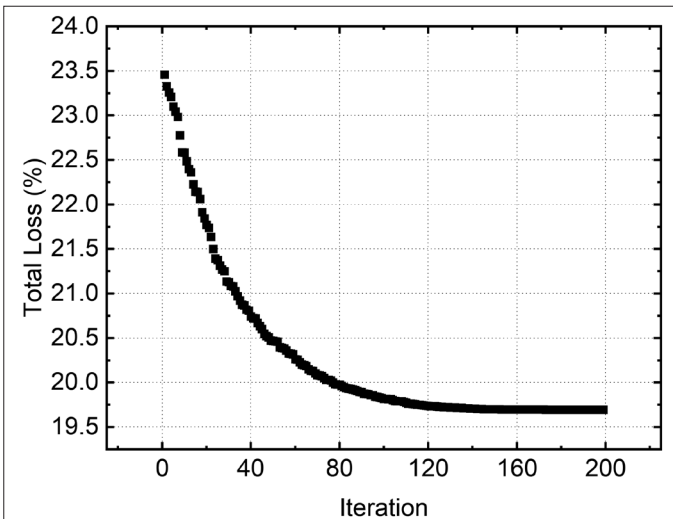


**Fig. 4.** Convergence curve of the surrogate optimization algorithm for total loss minimization.

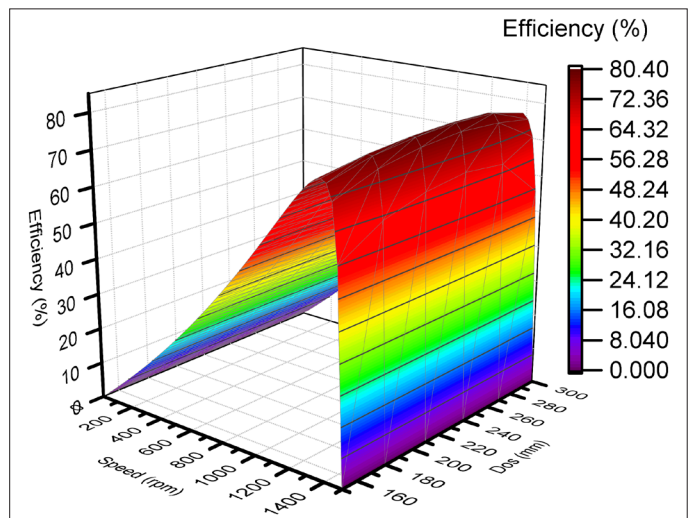


**Fig. 7.** Efficiency versus speed and  $D_{os}$  value.

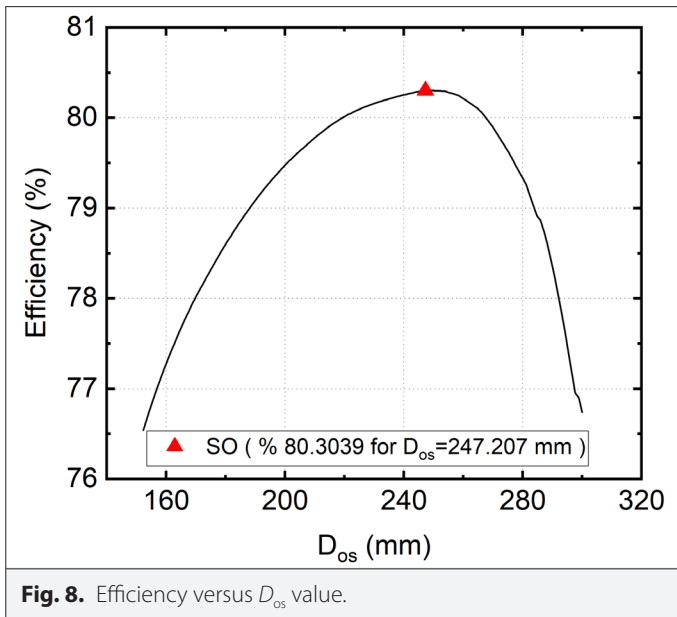


Fig. 8. Efficiency versus  $D_{os}$  value.

efficient case found by SO for this study is the one where the motor efficiency is 80.3% and  $K_d$  is 0.113.

#### IV. CONCLUSION

This study investigates the effects of asynchronous motor stator outer diameter and motor length on motor performance. The results show that the stator outer diameter value decreases as the  $K_d$  value increases. For this reason, the stator back iron height value has been increased, and the magnetic flux density value in these parts has been decreased.

As the motor length is reduced with the increase of the stator outer diameter value, there is no noticeable change in the motor weight. Considering that information, it is obvious that there is no serious change in motor cost since the stack pack volume of the motor is constant.

The study shows that the motor efficiency can be increased by 5.63% even if the motor cost does not change. Therefore, for all operation conditions, it is observed that the highest efficiency is obtained when the ratio of stator outer diameter to motor length is 8.85.

Optimization of the motor's physical parameters will be analyzed in more detail in future research to increase the energy efficiency and performance of the motor. In particular, the effect of these parameters under different load profiles and operating conditions will be investigated.

**Availability of Data and Materials:** The data that support the findings of this study are available on request from the corresponding author.

**Peer-review:** Externally peer-reviewed.

**Author Contributions:** Design – I.C., Y.O., M.C.A.; Supervision – Y.O., M.C.A.; Analysis – I.C., M.C.A.; Literature Review – I.C.; Writing – I.C.; Critical Review – Y.O., M.C.A.

**Declaration of Interests:** The authors have no conflict of interest to declare.

**Funding:** The authors declared that this study has received no financial support.

#### REFERENCES

1. P. Sakpal, and V. Mohale, "Design and analysis of a premium efficiency (ie3) induction motor," *Int. J. Res. Eng. Technol.*, vol. 5, no. 2, pp. 198–203, 2016.
2. International Electrotechnical Commission, "Test methods for determining quantities of equivalent circuit diagrams for three-phase low-voltage cage induction motors," in *Rotating Electrical Machines*, 2012. IEC 60034-28.
3. A. H. Bonnett, and G. C. Soukup, "Nema motor-generator standards for three-phase induction motors," *IEEE Ind. Appl. Mag.*, vol. 5, no. 3, pp. 49–63, 1999. [CrossRef]
4. A. Boglietti, A. Cavagnino, and S. Vaschetto, "Induction motor eu standards for efficiency evaluation: The scenario after iec 60034-2-1," *IECON-37th Annual Conference of the IEEE Industrial Electronics Society*, Melbourne, VIC, Australia, 2011, 2786–2791. [CrossRef]
5. International Electrotechnical Commission, "Standard Methods for Determining Losses and Efficiency from Tests (excluding machines for traction vehicles)," in *Rotating Electrical Machines*, 2014. IEC 60034-2-1
6. P. Vas, "Electrical Machines and Drives: A Space-Vector Theory Approach". Oxford: Oxford University Press, 1993.
7. S. Mallik et al., "Efficiency and cost optimized design of an induction motor using genetic algorithm," *IEEE Trans. Ind. Electron.*, vol. 64, no. 12, pp. 9854–9863, Dec. 2017. [CrossRef]
8. A. Marfoli, M. D. Di Nardo, M. Degano, C. Gerada, and W. Chen, "Rotor design optimization of squirrel cage induction motor-part i: Problem statement," *IEEE Trans. Energy Convers.*, vol. 36, no. 2, pp. 1271–1279, 2020. [CrossRef]
9. P. C. Krause, "Analysis of Electric Machinery and Drive Systems", vol. 2. IEEE Press, 2002, pp. 203–210.
10. T. A. Lipo, "Introduction to AC Machine Design". Chichester, UK: John Wiley & Sons, 2017.
11. I. Boldea, and S. A. Nasar, "Induction machines: An introduction," in *The Induction Machine Handbook*. Boca Raton, United States of America: CRC Press, 2002, p. 13.
12. I. Kuric, V. Tlach, M. Cisar, Z. Ságová, and I. Zajačko, "Examination of industrial robot performance parameters utilizing machine tool diagnostic methods" *Int. J. Adv. Robot. Syst.*, vol. 17, no. 1, 2020. [CrossRef]
13. V. Tlach, M. Cisar, I. Kuric, and I. Zajačko, "Determination of the industrial robot positioning performance," *MATEC Web of Conferences*, vol. 137. EDP Sciences, 2017. [CrossRef]
14. J. Pyrhonen, "Design of Rotating Electrical Machines". VCH Verlag: Wiley, 2013.
15. J. De Santiago, H. Bernhoff, B. Ekegård, S. Eriksson, S. Ferhatovic, R. Waters and M. Leijon, "Electrical motor drivelines in commercial all-electric vehicles: A review," *IEEE Trans. Veh. Technol.*, vol. 61, no. 2, pp. 475–484, 2011.
16. L. Di Leonardo, G. Fabri, A. Credo, M. Tursini, and M. Villani, "Impact of wire selection on the performance of an induction motor for automotive applications," *Energies*, vol. 15, no. 11, p. 3876, 2022. [CrossRef]
17. W. Tiecheng, Z. Ping, Z. Qianfan, and C. Shukang, "Design characteristics of the induction motor used for hybrid electric vehicle," in *2004 12th Symposium on Electromagnetic Launch Technology*, Snowbird, UT, USA, 2004.
18. Y. Guan, Z.-Q. Zhu, I. Afinow, and J.-C. Mipo, "Influence of machine design parameters on flux-weakening performance of induction machine for electrical vehicle application," *IET Electr. Syst. Transp.*, vol. 5, no. 1, pp. 43–52, 2015. [CrossRef]
19. M. J. Akhtar, and R. K. Behera, "Optimal design of stator and rotor slot of induction motor for electric vehicle applications," *IET Electr. Syst. Transp.*, vol. 9, no. 1, pp. 35–43, 2019. [CrossRef]
20. I. Chasiotis, Y. Karnavas, and F. Scullier, "Effect of rotor bars shape on the single-phase induction motors performance: An analysis toward their efficiency improvement," *Energies*, vol. 15, no. 3, p. 717, 2022. [CrossRef]
21. C. Mellak, J. Deuringer, and A. Muetze, "Impact of aspect ratios of solid rotor, large air gap induction motors on run-up time and energy input," *IEEE Trans. Ind. Appl.*, vol. 58, no. 5, pp. 6045–6056, 2022. [CrossRef]
22. A. Boglietti, A. Cavagnino, L. Ferraris, M. Lazzari, and G. Luparia, "No tooling cost process for induction motors energy efficiency improvements," *IEEE Trans. Ind. Appl.*, vol. 41, no. 3, pp. 808–816, 2005. [CrossRef]
23. E. B. Agamloh, A. Boglietti, and A. Cavagnino, "The incremental design efficiency improvement of commercially manufactured induction

- motors," *IEEE Trans. Ind. Appl.*, vol. 49, no. 6, pp. 2496–2504, 2013. [\[CrossRef\]](#)
24. L. Alberti, N. Bianchi, A. Boglietti, and A. Cavagnino, "Core axial lengthening as effective solution to improve the induction motor efficiency classes," *IEEE Trans. Ind. Appl.*, vol. 50, no. 1, pp. 218–225, 2013.
  25. J.-W. Kim, B.-T. Kim, and B. Kwon, "Optimal stator slot design of inverter-fed induction motor in consideration of harmonic losses," *IEEE Trans. Magn.*, vol. 41, no. 5, pp. 2012–2015, 2005. [\[CrossRef\]](#)
  26. D. Zhang, C. S. Park, and C. S. Koh, "A new optimal design method of rotor slot of three-phase squirrel cage induction motor for nema class d speed-torque characteristic using multi-objective optimization algorithm," *IEEE Trans. Magn.*, vol. 48, no. 2, pp. 879–882, 2012. [\[CrossRef\]](#)
  27. M. Sága, M. Vaško, M. Handrik, and P. Kopas, "Contribution to random vibration numerical simulation and optimisation of nonlinear mechanical systems," *SJSUTST*, vol. 103, 143–154, 2019. [\[CrossRef\]](#)
  28. S. Jurkovic, K. M. Rahman, J. C. Morgante, and P. J. Savagian, "Induction machine design and analysis for general motors e-assist electrification technology," *IEEE Trans. Ind. Appl.*, vol. 51, no. 1, pp. 631–639, 2014. [\[CrossRef\]](#)
  29. G. Liuzzi, S. Lucidi, F. Parasiliti, and M. Villani, "Multiobjective optimization techniques for the design of induction motors," *IEEE Trans. Magn.*, vol. 39, no. 3, pp. 1261–1264, 2003. [\[CrossRef\]](#)
  30. J. P. Wiecek, O. Gol, and Z. Michalewicz, "An evolutionary algorithm for the optimal design of induction motors," *IEEE Trans. Magn.*, vol. 34, no. 6, pp. 3882–3887, 1998. [\[CrossRef\]](#)
  31. M. Tumbek, Y. Oner, and S. Kesler, "Optimal design of induction motor with multi-parameter by fem method," in 2015 9th International Conference on Electrical and Electronics Engineering (ELECO), Bursa, Türkiye, 2015. [\[CrossRef\]](#)
  32. S. V. Umredkar, R. K. Keshri, V. B. Borghate, and M. M. Renge, "Dynamic configuration of slot per pole per phase of an induction motor," In 2022 IEEE International Conference on Power Electronics, Drives and Energy Systems (PEDES), Jaipur, India, 2022, pp. 1–6. [\[CrossRef\]](#)
  33. M. Mohan, H. Vallecha, S. Singh, A. Nayyar, A. Kumar, and N. Singh, "A comparative study on performance of 3kW induction motor with different shapes of stator slots," *Int. J. Eng. Sci. Technol.*, vol. 4, no. 6, pp. 2446–2452, 2012.
  34. A. Yetkin, A. Canakoglu, A. Gün, M. Turan, and B. Cevher, "Effect of the induction motor stator outer/innerdiameter ratio on the motor performance," In 7th International Conference on Advanced Technologies, Antalya, Türkiye, 2018.
  35. M. Nakhaei, and R. Roshanfekar, "Optimal design of 3-phase squirrel cage induction motors using genetic algorithm based on the motor efficiency and economic evaluation of the optimal model," *Balkan J. Electr. Comput. Eng.*, vol. 9, no. 1, pp. 59–68, 2021.
  36. N. V. Queipo, R. T. Haftka, W. Shyy, T. Goel, R. Vaidyanathan, and P. K. Tucker, "Surrogate-based analysis and optimization," *Prog. Aerosp. Sci.*, vol. 41, no. 1, pp. 1–28, 2005. [\[CrossRef\]](#)
  37. T. Simpson, V. Toropov, V. Balabanov, and F. Viana, "Design and analysis of computer experiments in multidisciplinary design optimization: A review of how far we have come-or not," In 12th AIAA/ISSMO multidisciplinary analysis and optimization conference, p. vol. 5802, 2008. [\[CrossRef\]](#)



İbrahim Çelik received an M.Sc in machine engineering from Afyon Kocatepe University in 2019. He is a research assistant in the Mechatronic Engineering Department at Afyon Kocatepe University, Afyonkarahisar, Türkiye.



Yüksel Oğuz received his M. Sc and Ph.D. in Electrical Education from the Marmara University, Institute for Graduate Studies in Pure and Applied Sciences, between 2000 and 2007. He is working as a Professor in the Electrical and Electronic Engineering Department at Afyon Kocatepe University. His research interests include control systems, automatic applications, electrical machines, and intelligent control systems.



M. Caner Aküner received his M. Sc and Ph.D. in Electrical Education from the Marmara University, Institute for Graduate Studies in Pure and Applied Sciences, between 1990 and 1999. He is currently a Professor in the Mechatronic Engineering Department at Marmara University.